

1 A comparison of nine machine learning models based on an  
2 expanded mutagenicity dataset and their application for  
3 predicting pyrrolizidine alkaloid mutagenicity

4 Christoph Helma<sup>\*1</sup>, Verena Schöning<sup>4</sup>, Philipp Boss<sup>3</sup>, and Jürgen Drewe<sup>2</sup>

5 <sup>1</sup>in silico toxicology gmbh, Rastatterstrasse 41, 4057 Basel, Switzerland

6 <sup>2</sup>Zeller AG, Seeblickstrasse 4, 8590 Romanshorn, Switzerland

7 <sup>3</sup>Berlin Institute for Medical Systems Biology, Max Delbrück Center for Molecular  
8 Medicine in the Helmholtz Association, Robert-Rössle-Strasse 10, Berlin, 13125, Germany

9 <sup>4</sup>Clinical Pharmacology and Toxicology, Department of General Internal Medicine,  
10 Bern University Hospital, University of Bern, Inselspital, 3010 Bern, Switzerland

11 <sup>\*</sup> Correspondence: Christoph Helma <helma@in-silico.ch>

12 Random forest, support vector machine, logistic regression, neural  
13 networks and k-nearest neighbor (**lazar**) algorithms, were applied to new  
14 *Salmonella* mutagenicity dataset with 8309 unique chemical structures. The  
15 best prediction accuracies in 10-fold-crossvalidation were obtained with  
16 **lazar** models and MolPrint2D descriptors, that gave accuracies (84%)  
17 similar to the interlaboratory variability of the Ames test.

18 **TODO:** PA results

19 **Introduction**

20 **TODO:** rationale for investigation

21 The main objectives of this study were

- 22 • to generate a new mutagenicity training dataset, by combining the most compre-  
23 hensive public datasets
- 24 • to compare the performance of MolPrint2D (*MP2D*) fingerprints with PaDEL de-  
25 scriptors
- 26 • to compare the performance of global QSAR models (random forests (*RF*), support  
27 vector machines (*SVM*), logistic regression (*LR*), neural nets (*NN*)) with local  
28 models (*lazar*)
- 29 • to apply these models for the prediction of pyrrolizidine alkaloid mutagenicity

## 30 **Materials and Methods**

### 31 **Data**

#### 32 **Mutagenicity training data**

33 An identical training dataset was used for all models. The training dataset was compiled  
34 from the following sources:

- 35 • Kazius/Bursi Dataset (4337 compounds, Kazius, McGuire, and Bursi (2005)):  
36 [http://cheminformatics.org/datasets/bursi/cas\\_4337.zip](http://cheminformatics.org/datasets/bursi/cas_4337.zip)
- 37 • Hansen Dataset (6513 compounds, Hansen et al. (2009)): [http://doc.ml.tu-berlin.](http://doc.ml.tu-berlin.de/toxbenchmark/Mutagenicity_N6512.csv)  
38 [de/toxbenchmark/Mutagenicity\\_N6512.csv](http://doc.ml.tu-berlin.de/toxbenchmark/Mutagenicity_N6512.csv)
- 39 • EFSA Dataset (695 compounds EFSA (2016)): [https://data.europa.eu/euodp/](https://data.europa.eu/euodp/data/storage/f/2017-0719T142131/GENOTOX%20data%20and%20dictionary.xls)  
40 [data/storage/f/2017-0719T142131/GENOTOX%20data%20and%20dictionary.xls](https://data.europa.eu/euodp/data/storage/f/2017-0719T142131/GENOTOX%20data%20and%20dictionary.xls)

41 Mutagenicity classifications from Kazius and Hansen datasets were used without further  
42 processing. To achieve consistency with these datasets, EFSA compounds were classified  
43 as mutagenic, if at least one positive result was found for TA98 or T100 Salmonella

44 strains.

45 Dataset merges were based on unique SMILES (*Simplified Molecular Input Line Entry*  
46 *Specification*) strings of the compound structures. Duplicated experimental data with  
47 the same outcome was merged into a single value, because it is likely that it originated  
48 from the same experiment. Contradictory results were kept as multiple measurements  
49 in the database. The combined training dataset contains 8309 unique structures.

50 Source code for all data download, extraction and merge operations is pub-  
51 licly available from the git repository <https://git.in-silico.ch/mutagenicity-paper>  
52 under a GPL3 License. The new combined dataset can be found at <https://git.in-silico.ch/mutagenicity-paper/data/mutagenicity.csv>.  
53

#### 54 **Pyrrolizidine alkaloid (PA) dataset**

55 The testing dataset consisted of 602 different PAs.

56 The PA dataset was created from five independent, necine base substructure searches in  
57 PubChem (<https://pubchem.ncbi.nlm.nih.gov/>) and compared to the PAs listed in the  
58 EFSA publication EFSA (2011) and the book by Mattocks Mattocks (1986), to ensure,  
59 that all major PAs were included. PAs mentioned in these publications which were  
60 not found in the downloaded substances were searched individually in PubChem and,  
61 if available, downloaded separately. Non-PA substances, duplicates, and isomers were  
62 removed from the files, but artificial PAs, even if unlikely to occur in nature, were kept.  
63 The resulting PA dataset comprised a total of 602 different PAs.

64 The PAs in the dataset were classified according to structural features. A total of 9  
65 different structural features were assigned to the necine base, modifications of the necine  
66 base and to the necic acid:

67 For the necine base, the following structural features were chosen:

- 68 • Retronecine-type (1,2-unsaturated necine base)
- 69 • Otonecine-type (1,2-unsaturated necine base)
- 70 • Platynecine-type (1,2-saturated necine base)

71 For the modifications of the necine base, the following structural features were chosen:

- 72 • N-oxide-type
- 73 • Tertiary-type (PAs which were neither from the N-oxide- nor DHP-type)
- 74 • DHP-type (pyrrolic ester)

75 For the necic acid, the following structural features were chosen:

- 76 • Monoester-type
- 77 • Open-ring diester-type
- 78 • Macrocyclic diester-type

79 The compilation of the PA dataset is described in detail in Schöning et al. (2017).

## 80 **Descriptors**

### 81 **MolPrint2D (*MP2D*) fingerprints**

82 MolPrint2D fingerprints (O’Boyle et al. (2011)) use atom environments as molecular  
83 representation. They determine for each atom in a molecule, the atom types of its  
84 connected atoms to represent their chemical environment. This resembles basically the  
85 chemical concept of functional groups.

86 In contrast to predefined lists of fragments (e.g. FP3, FP4 or MACCs fingerprints) or  
87 descriptors (e.g PaDEL) they are generated dynamically from chemical structures. This  
88 has the advantage that they can capture substructures of toxicological relevance that  
89 are not included in other descriptors.

90 Chemical similarities (e.g. Tanimoto indices) can be calculated very efficiently with Mol-

Print2D fingerprints. Using them as descriptors for global models leads however to huge, sparsely populated matrices that cannot be handled with traditional machine learning algorithms. In our experiments none of the R and Tensorflow algorithms was capable to use them as descriptors.

MolPrint2D fingerprints were calculated with the OpenBabel cheminformatics library (O’Boyle et al. (2011)).

### PaDEL descriptors

Molecular 1D and 2D descriptors were calculated with the PaDEL-Descriptors program (<http://www.yapcwsoft.com> version 2.21, Yap (2011)).

As the training dataset contained over 8309 instances, it was decided to delete instances with missing values during data pre-processing. Furthermore, substances with equivocal outcome were removed. The final training dataset contained 8080 instances with known mutagenic potential.

During feature selection, descriptors with near zero variance were removed using ‘*NearZero Var*’-function (package ‘caret’). If the percentage of the most common value was more than 90% or when the frequency ratio of the most common value to the second most common value was greater than 95:5 (e.g. 95 instances of the most common value and only 5 or less instances of the second most common value), a descriptor was classified as having a near zero variance. After that, highly correlated descriptors were removed using the ‘*findCorrelation*’-function (package ‘caret’) with a cut-off of 0.9. This resulted in a training dataset with 516 descriptors. These descriptors were scaled to be in the range between 0 and 1 using the ‘*preProcess*’-function (package ‘caret’). The scaling routine was saved in order to apply the same scaling on the testing dataset. As these three steps did not consider the dependent variable (experimental mutagenicity), it was decided that they do not need to be included in the cross-validation of the model. To

116 further reduce the number of features, a LASSO (*least absolute shrinkage and selection*  
117 *operator*) regression was performed using the ‘*glmnet*’-function (package ‘*glmnet*’). The  
118 reduced dataset was used for the generation of the pre-trained models.

119 PaDEL descriptors were used in global (RF, SVM, LR, NN) and local (**lazar**) models.

## 120 **Algorithms**

### 121 **lazar**

122 **lazar** (*lazy structure activity relationships*) is a modular framework for read-across model  
123 development and validation. It follows the following basic workflow: For a given chemical  
124 structure **lazar**:

- 125 • searches in a database for similar structures (neighbours) with experimental data,
- 126 • builds a local QSAR model with these neighbours and
- 127 • uses this model to predict the unknown activity of the query compound.

128 This procedure resembles an automated version of read across predictions in toxicology,  
129 in machine learning terms it would be classified as a k-nearest-neighbour algorithm.

130 Apart from this basic workflow, **lazar** is completely modular and allows the researcher to  
131 use arbitrary algorithms for similarity searches and local QSAR (*Quantitative structure–*  
132 *activity relationship*) modelling. Algorithms used within this study are described in the  
133 following sections.

### 134 **Neighbour identification**

135 Utilizing this modularity, similarity calculations were based both on MolPrint2D finger-  
136 prints and on PaDEL descriptors.

137 For MolPrint2D fingerprints chemical similarity between two compounds *a* and *b* is

expressed as the proportion between atom environments common in both structures  $A \cap B$  and the total number of atom environments  $A \cup B$  (Jaccard/Tanimoto index).

$$sim = \frac{|A \cap B|}{|A \cup B|}$$

For PaDEL descriptors chemical similarity between two compounds  $a$  and  $b$  is expressed as the cosine similarity between the descriptor vectors  $A$  for  $a$  and  $B$  for  $b$ .

$$sim = \frac{A \cdot B}{|A||B|}$$

Threshold selection is a trade-off between prediction accuracy (high threshold) and the number of predictable compounds (low threshold). As it is in many practical cases desirable to make predictions even in the absence of closely related neighbours, we follow a tiered approach:

- First a similarity threshold of 0.5 is used to collect neighbours, to create a local QSAR model and to make a prediction for the query compound. This are predictions with *high confidence*.
- If any of these steps fails, the procedure is repeated with a similarity threshold of 0.2 and the prediction is flagged with a warning that it might be out of the applicability domain of the training data (*low confidence*).
- Similarity thresholds of 0.5 and 0.2 are the default values chosen by the software developers and remained unchanged during the course of these experiments.

Compounds with the same structure as the query structure are automatically eliminated from neighbours to obtain unbiased predictions in the presence of duplicates.

## Local QSAR models and predictions

157 Only similar compounds (neighbours) above the threshold are used for local QSAR  
 158 models. In this investigation, we are using a weighted majority vote from the neigh-  
 159 bour’s experimental data for mutagenicity classifications. Probabilities for both classes  
 160 (mutagenic/non-mutagenic) are calculated according to the following formula and the  
 161 class with the higher probability is used as prediction outcome.

$$p_c = \frac{\sum \text{sim}_{n,c}}{\sum \text{sim}_n}$$

162  $p_c$  Probability of class c (e.g. mutagenic or non-mutagenic)

163  $\sum \text{sim}_{n,c}$  Sum of similarities of neighbours with class c

164  $\sum \text{sim}_n$  Sum of all neighbours

## 165 **Applicability domain**

166 The applicability domain (AD) of **lazar** models is determined by the structural diver-  
 167 sity of the training data. If no similar compounds are found in the training data no  
 168 predictions will be generated. Warnings are issued if the similarity threshold had to be  
 169 lowered from 0.5 to 0.2 in order to enable predictions. Predictions without warnings  
 170 can be considered as close to the applicability domain (*high confidence*) and predictions  
 171 with warnings as more distant from the applicability domain (*low confidence*). Quantita-  
 172 tive applicability domain information can be obtained from the similarities of individual  
 173 neighbours.

## 174 **Availability**

- 175 • **lazar** experiments for this manuscript: <https://git.in-silico.ch/mutagenicity-paper>  
 176 (source code, GPL3)
- 177 • **lazar** framework: <https://git.in-silico.ch/lazar> (source code, GPL3)



- 178 • **lazar** GUI: <https://git.in-silico.ch/lazar-gui> (source code, GPL3)
- 179 • Public web interface: <https://lazar.in-silico.ch>

## 180 **R Random Forest, Support Vector Machines, and Deep Learning**

181 The RF, SVM, and DL models were generated using the R software (R-project for  
182 Statistical Computing, <https://www.r-project.org/>; version 3.3.1), specific R packages  
183 used are identified for each step in the description below.

### 184 **Random Forest (*RF*)**

185 For the RF model, the '*randomForest*'-function (package '*randomForest*') was used. A  
186 forest with 1000 trees with maximal terminal nodes of 200 was grown for the prediction.

### 187 **Support Vector Machines (*SVM*)**

188 The '*svm*'-function (package 'e1071') with a *radial basis function kernel* was used for the  
189 SVM model.

190 **TODO: Verena, Phillip** Sollen wir die DL Modelle ebenso wie die Tensorflow als  
191 Neural Nets (NN) bezeichnen?

### 192 **Deep Learning**

193 The DL model was generated using the '*h2o.deeplearning*'-function (package '*h2o*'). The  
194 DL contained four hidden layer with 70, 50, 50, and 10 neurons, respectively. Other  
195 hyperparameter were set as follows:  $l1=1.0E-7$ ,  $l2=1.0E-11$ ,  $\epsilon = 1.0E-10$ ,  $\rho =$   
196  $0.8$ , and  $\text{quantile\_alpha} = 0.5$ . For all other hyperparameter, the default values were  
197 used. Weights and biases were in a first step determined with an unsupervised DL model.  
198 These values were then used for the actual, supervised DL model.

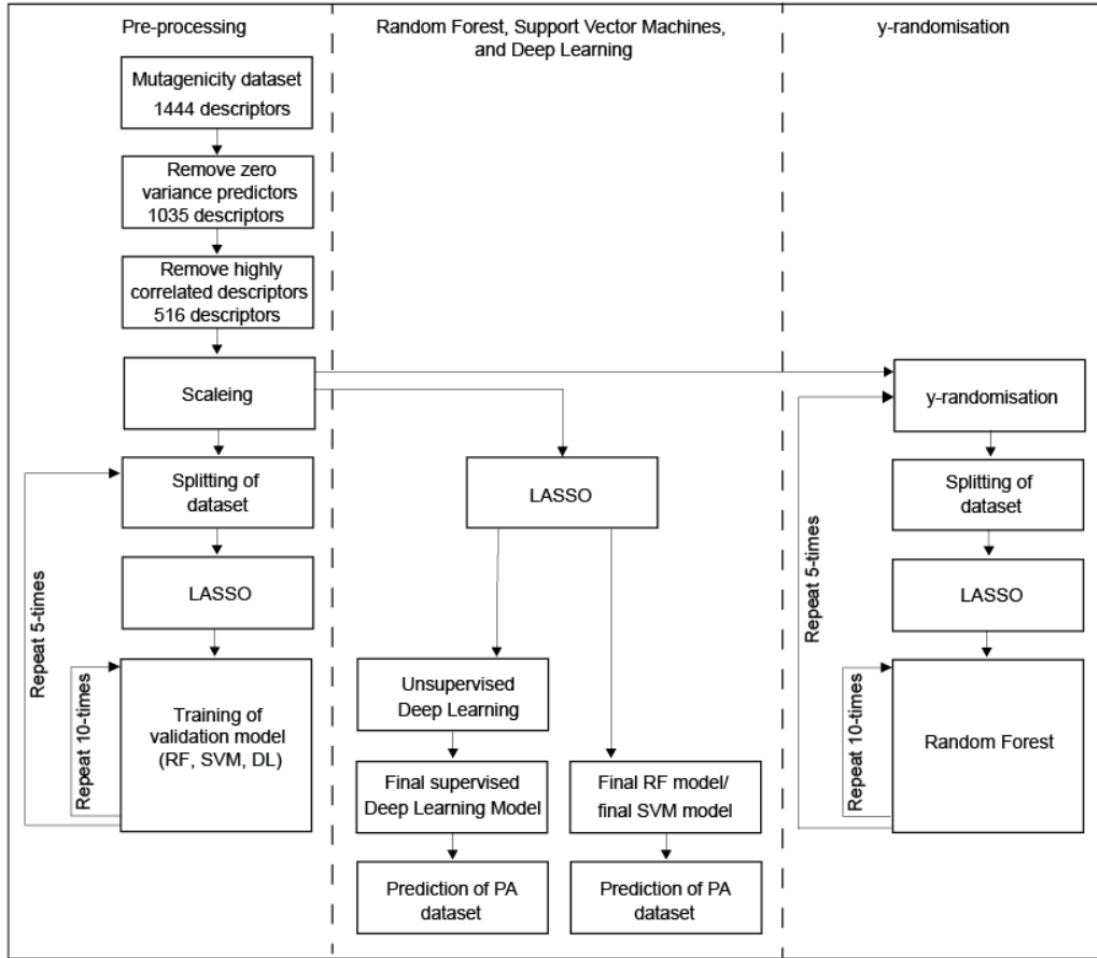


Figure 1: Flowchart of the generation and validation of the models generated in R-project

199 To validate these models, an internal cross-validation approach was chosen. The training  
 200 dataset was randomly split in training data, which contained 95% of the data, and  
 201 validation data, which contain 5% of the data. A feature selection with LASSO on the  
 202 training data was performed, reducing the number of descriptors to approximately 100.  
 203 This step was repeated five times. Based on each of the five different training data,  
 204 the predictive models were trained and the performance tested with the validation data.  
 205 This step was repeated 10 times.

## 206 **Applicability domain**

207 **TODO: Verena:** Mit welchen Deskriptoren hast Du den Jaccard index berechnet?  
208 Fuer den Jaccard index braucht man binaere Deskriptoren (zB MP2D), mit PaDEL  
209 Deskriptoren koennte man zB eine euklidische oder cosinus Distanz berechnen.

210 The AD of the training dataset and the PA dataset was evaluated using the Jaccard  
211 distance. A Jaccard distance of ‘0’ indicates that the substances are similar, whereas a  
212 value of ‘1’ shows that the substances are different. The Jaccard distance was below 0.2  
213 for all PAs relative to the training dataset. Therefore, PA dataset is within the AD of  
214 the training dataset and the models can be used to predict the genotoxic potential of  
215 the PA dataset.

## 216 **Availability**

217 R scripts for these experiments can be found in [https://git.in-silico.ch/mutagenicity-](https://git.in-silico.ch/mutagenicity-paper/scripts/R)  
218 [paper/scripts/R](https://git.in-silico.ch/mutagenicity-paper/scripts/R).

## 219 **Tensorflow models**

220 Data pre-processing was done by rank transformation using the ‘*QuantileTransformer*’  
221 procedure. A sequential model has been used. Four layers have been used: input layer,  
222 two hidden layers (with 12, 8 and 8 nodes, respectively) and one output layer. For the  
223 output layer, a sigmoidal activation function and for all other layers the ReLU (‘*Rectified*  
224 *Linear Unit*’) activation function was used. Additionally, a  $L^2$ -penalty of 0.001 was used  
225 for the input layer. For training of the model, the ADAM algorithm was used to minimise  
226 the cross-entropy loss using the default parameters of Keras. Training was performed  
227 for 100 epochs with a batch size of 64. The model was implemented with Python 3.6  
228 and Keras.

229 **TODO: Philipp** Ich hab die alten Ergebnisse mit feature selection weggelassen, ist das  
230 ok? Dann muesste auch dieser Absatz gestrichen werden, oder?

231 **TODO: Philipp** Kannst Du bitte die folgenden Absaetze ergaenzen

232 **Random forests (*RF*)**

233 **Logistic regression (SGD) (*LR-sgd*)**

234 **Logistic regression (scikit) (*LR-scikit*)**

235 **TODO: Philipp, Verena** DL oder NN?

236 **Neural Nets (*NN*)**

237 Alternatively, a DL model was established with Python-based Tensorflow program ([https:](https://www.tensorflow.org/)  
238 [//www.tensorflow.org/](https://www.tensorflow.org/)) using the high-level API Keras ([https://www.tensorflow.org/](https://www.tensorflow.org/guide/keras)  
239 [guide/keras](https://www.tensorflow.org/guide/keras)) to build the models.

240 Tensorflow models used the same PaDEL descriptors as the R models.

241 **Validation**

242 10-fold cross-validation was used for all Tensorflow models.

243 **Availability**

244 Jupyter notebooks for these experiments can be found in [https://git.in-silico.ch/mutagenicity-](https://git.in-silico.ch/mutagenicity-paper/scripts/tensorflow)  
245 [paper/scripts/tensorflow](https://git.in-silico.ch/mutagenicity-paper/scripts/tensorflow).

## Results

### 10-fold crossvalidations

Crossvalidation results are summarized in the following tables: Table 1 shows **lazar** results with MolPrint2D and PaDEL descriptors, Table 2 R results and Table 3 Tensorflow results.

Table 1: Summary of **lazar** crossvalidation results (all/high confidence predictions)

	MP2D	PaDEL
Accuracy	0.82/0.84	0.58/0.58
True positive rate/Sensitivity	0.85/0.89	0.32/0.32
True negative rate/Specificity	0.78/0.79	0.79/0.79
Positive predictive value/Precision	0.8/0.83	0.56/0.56
Negative predictive value	0.84/0.85	0.59/0.59
Nr. predictions	7781/5890	4089/4081

Table 2: Summary of R crossvalidation results

	RF	SVM	DL
Accuracy	0.64	0.61	0.56
True positive rate/Sensitivity	0.56	0.56	0.88
True negative rate/Specificity	0.71	0.67	0.24
Positive predictive value/Precision	0.66	0.62	0.53
Negative predictive value	0.62	0.61	0.67
Nr. predictions	8070	8070	8070

Table 3: Summary of tensorflow crossvalidation results

	RF	LR-sgd	LR-scikit	NN
Accuracy	0.64	0.62	0.63	0.63
True positive rate/Sensitivity	0.59	0.6	0.62	0.61
True negative rate/Specificity	0.7	0.65	0.63	0.64
Positive predictive value/Precision	0.66	0.63	0.62	0.63
Negative predictive value	0.63	0.62	0.63	0.63
Nr. predictions	8080	8080	8080	8080

Figure 2 depicts the position of all crossvalidation results in receiver operating characteristic (ROC) space.

Confusion matrices for all models are available from the git repository <https://git.in-silico.ch/mutagenicity-paper/10-fold-crossvalidations/confusion-matrices/>, individual predictions can be found in <https://git.in-silico.ch/mutagenicity-paper/10-fold-crossvalidations/predictions/>.

The most accurate crossvalidation predictions have been obtained with standard **lazar** models using MolPrint2D descriptors (0.84 for predictions with high confidence, 0.82 for all predictions). Models utilizing PaDEL descriptors have generally lower accuracies ranging from 0.56 (R deep learning) to 0.64 (R/Tensorflow random forests). Sensitivity and specificity is generally well balanced with the exception of **lazar**-PaDEL (low sensitivity) and R deep learning (low specificity) models.

### **Pyrrolizidine alkaloid mutagenicity predictions**

Mutagenicity predictions from all investigated models for 602 pyrrolizidine alkaloids (PAs) are shown in Table 4. A CSV table with all predictions can be downloaded from

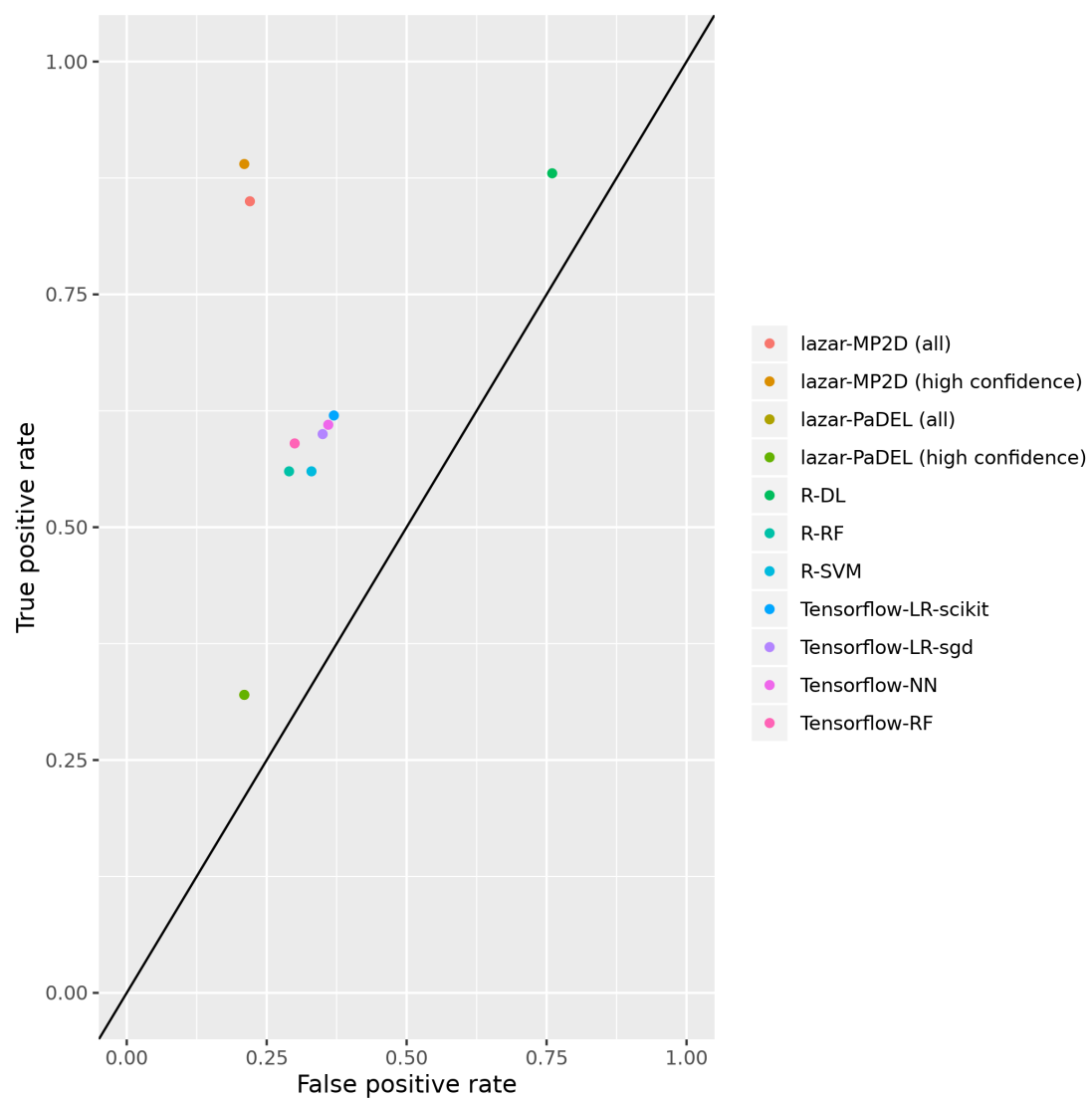


Figure 2: ROC plot of crossvalidation results.

266 <https://git.in-silico.ch/mutagenicity-paper/tables/pa-table.csv>

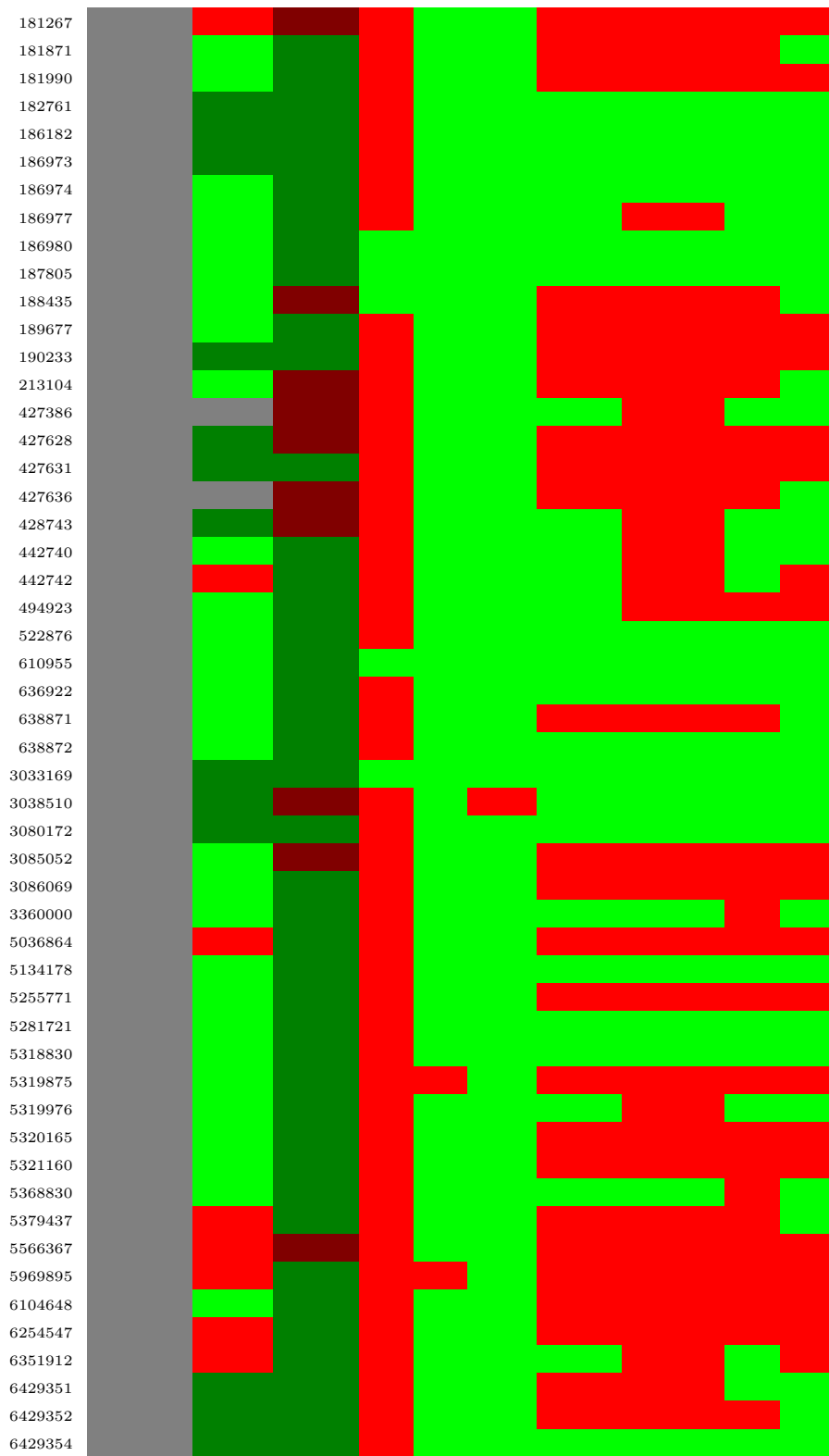
267 **TODO Verena und Philipp** Koennt Ihr bitte stichprobenweise die Tabelle ueberprue-  
 268 fen

Table 4: Summary of pyrrolizidine alkaloid predictions: red: mutagen, green: non-mutagen, grey: no prediction, dark red/green: low confidence

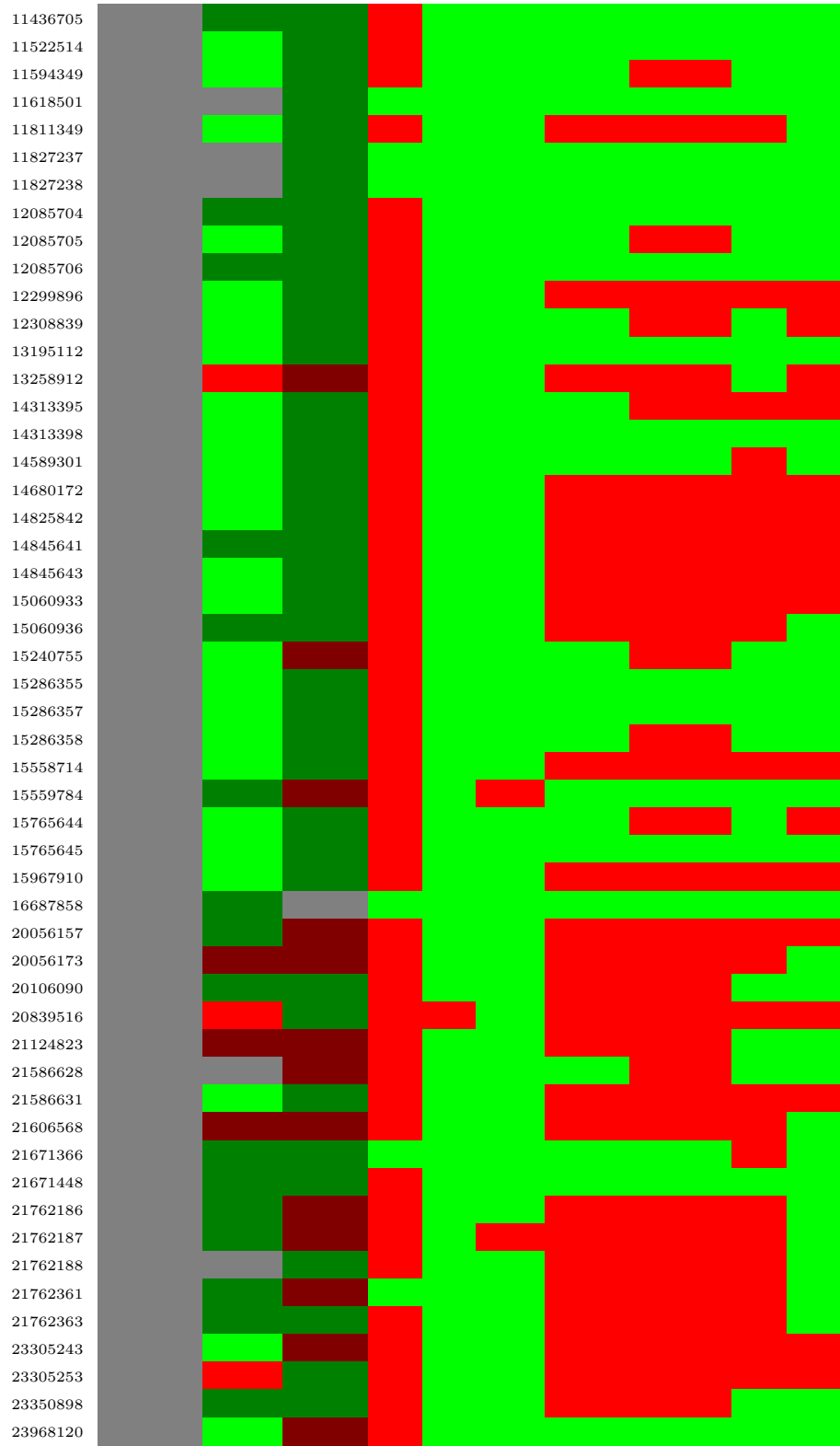
PubChem		lazar			R		Tensorflow			
CID	Measured	MP2D	PaDEL	DL	RF	SVM	LR-sgd	LR-scikit	NN	RF
9415										
5281743										
73614										
119040										
280564										
5280906										
5281733										
5281734										
5281744										
5281756										
5380876										
21606566										
613201										
5281750										
5355258										
9341										
10198										
577603										
99322										
185716										
442726										
5281753										
5281754										
6269253										
6440301										
6440889										
6441178										
12308873										
15120074										
15736564										
76957522										
98222										
197173										
259727										
268949										
279070										
323256										
333106										
333468										
333469										
340066										

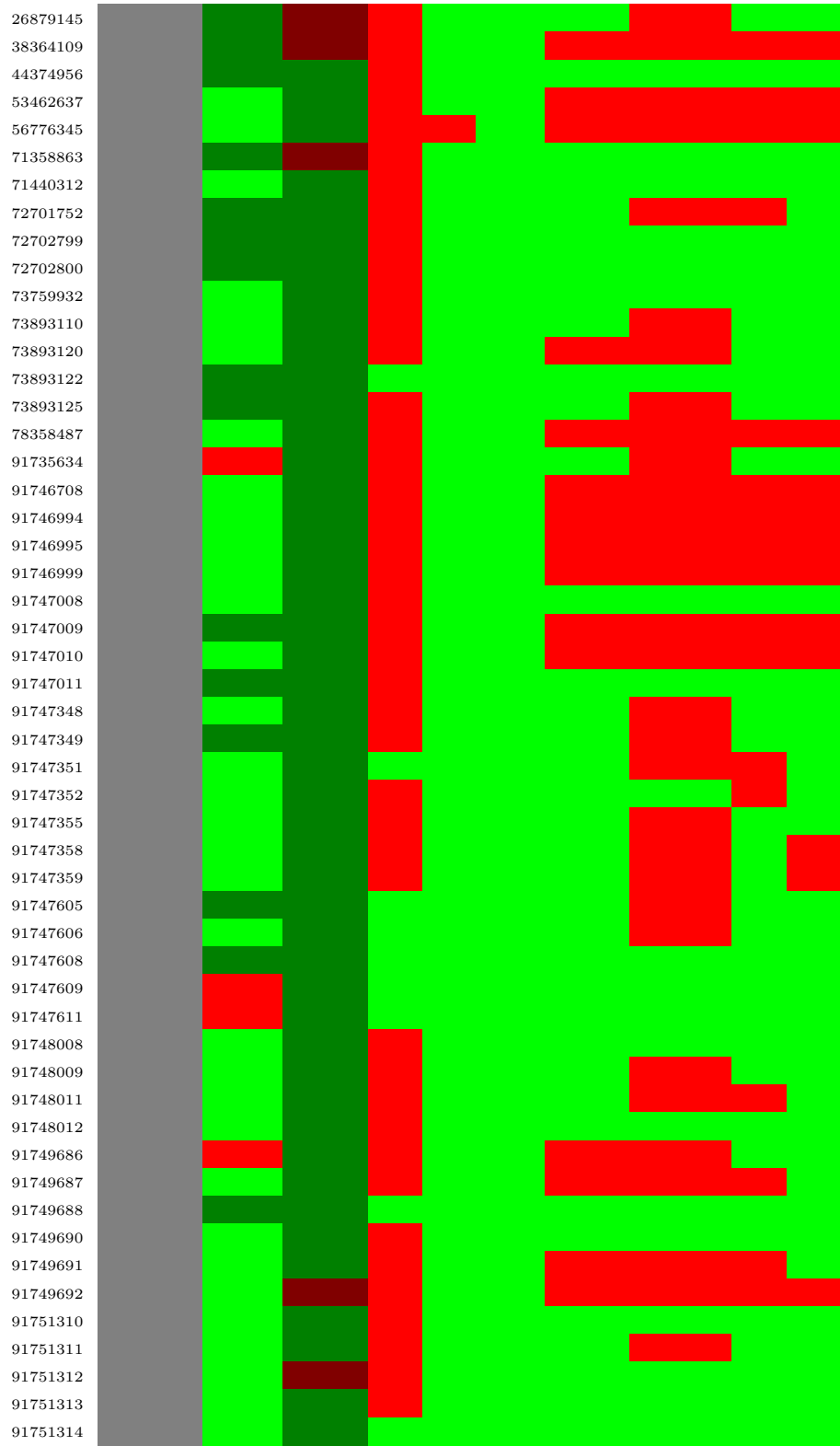






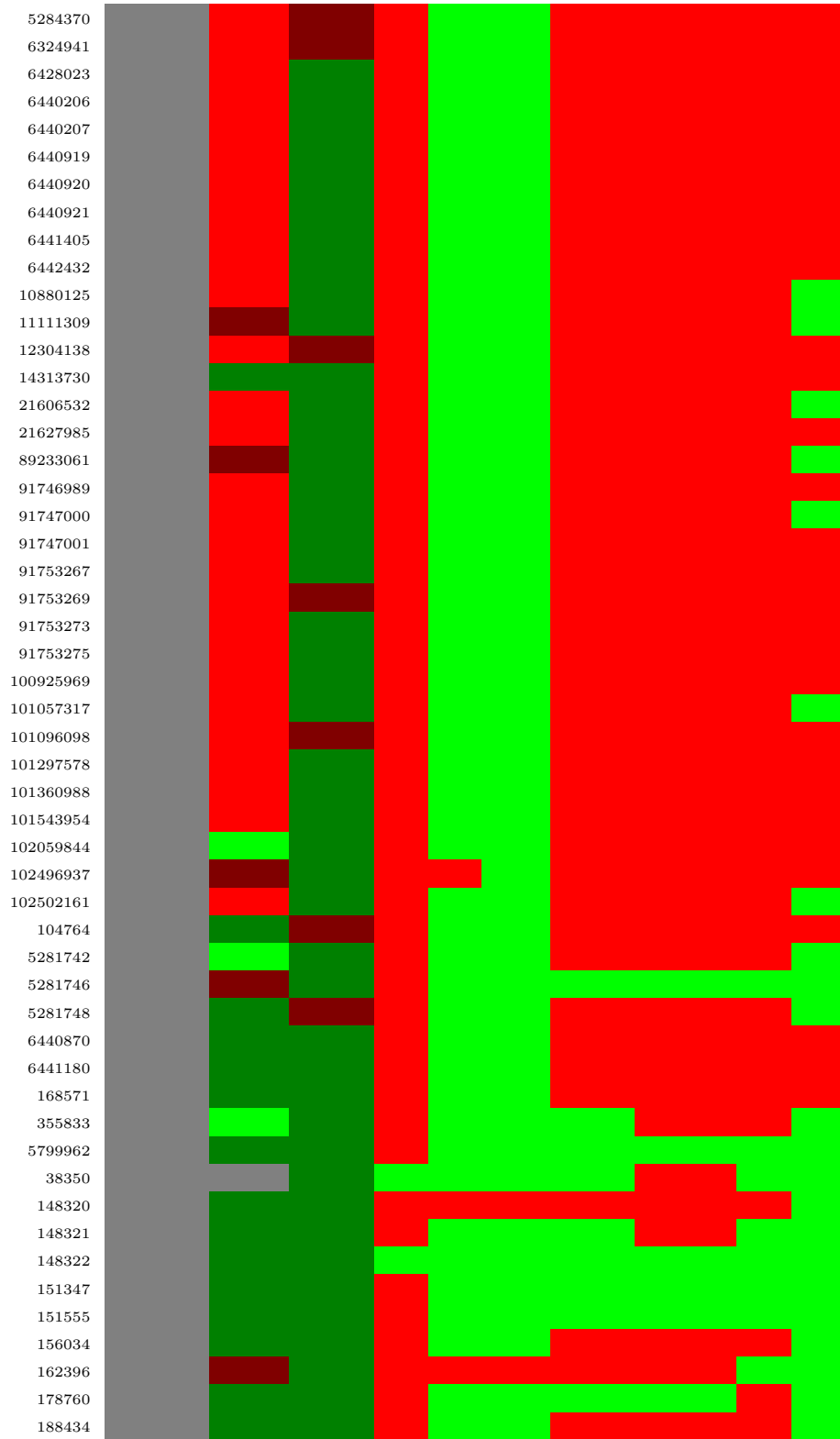




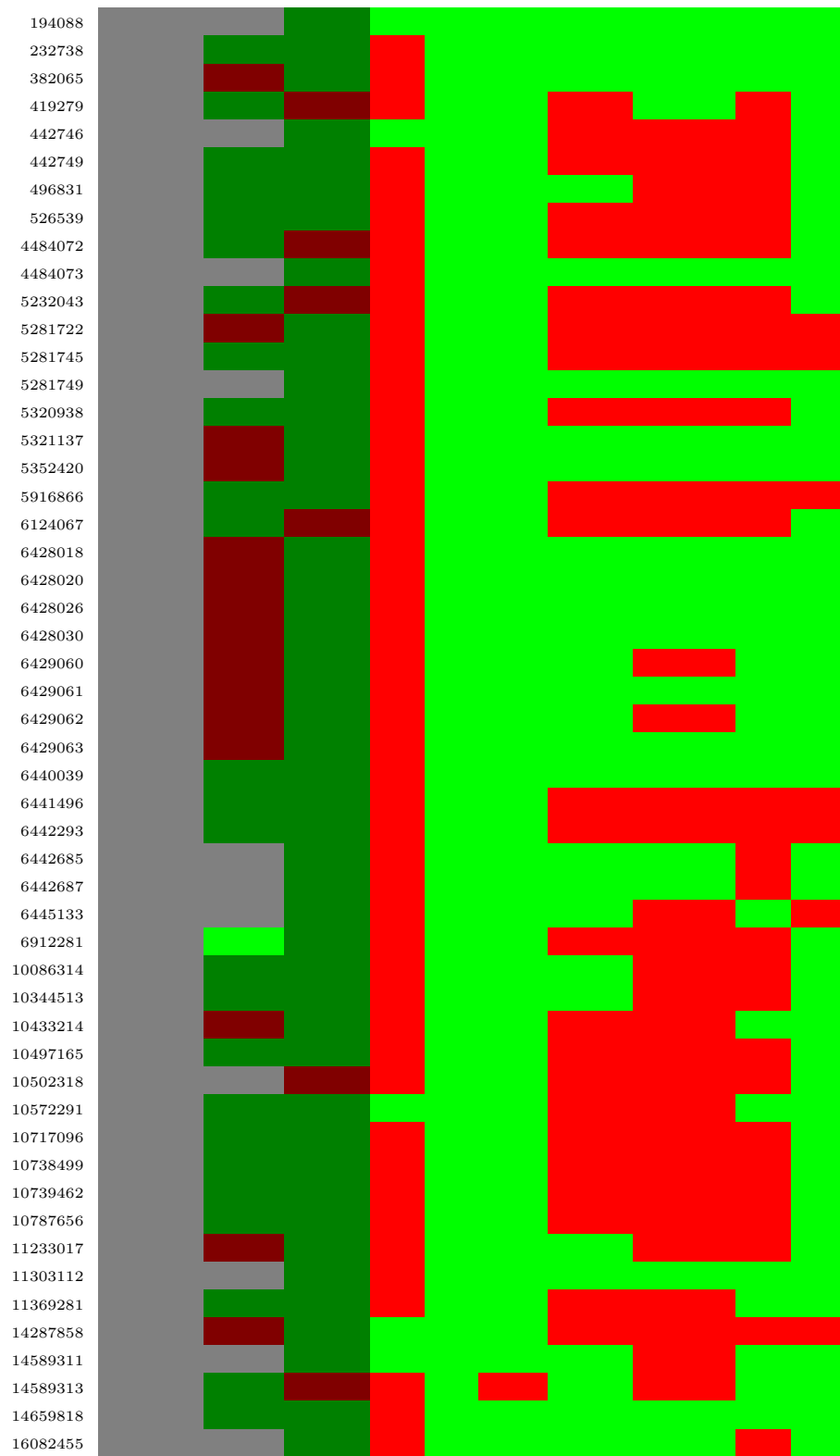


[illegible]

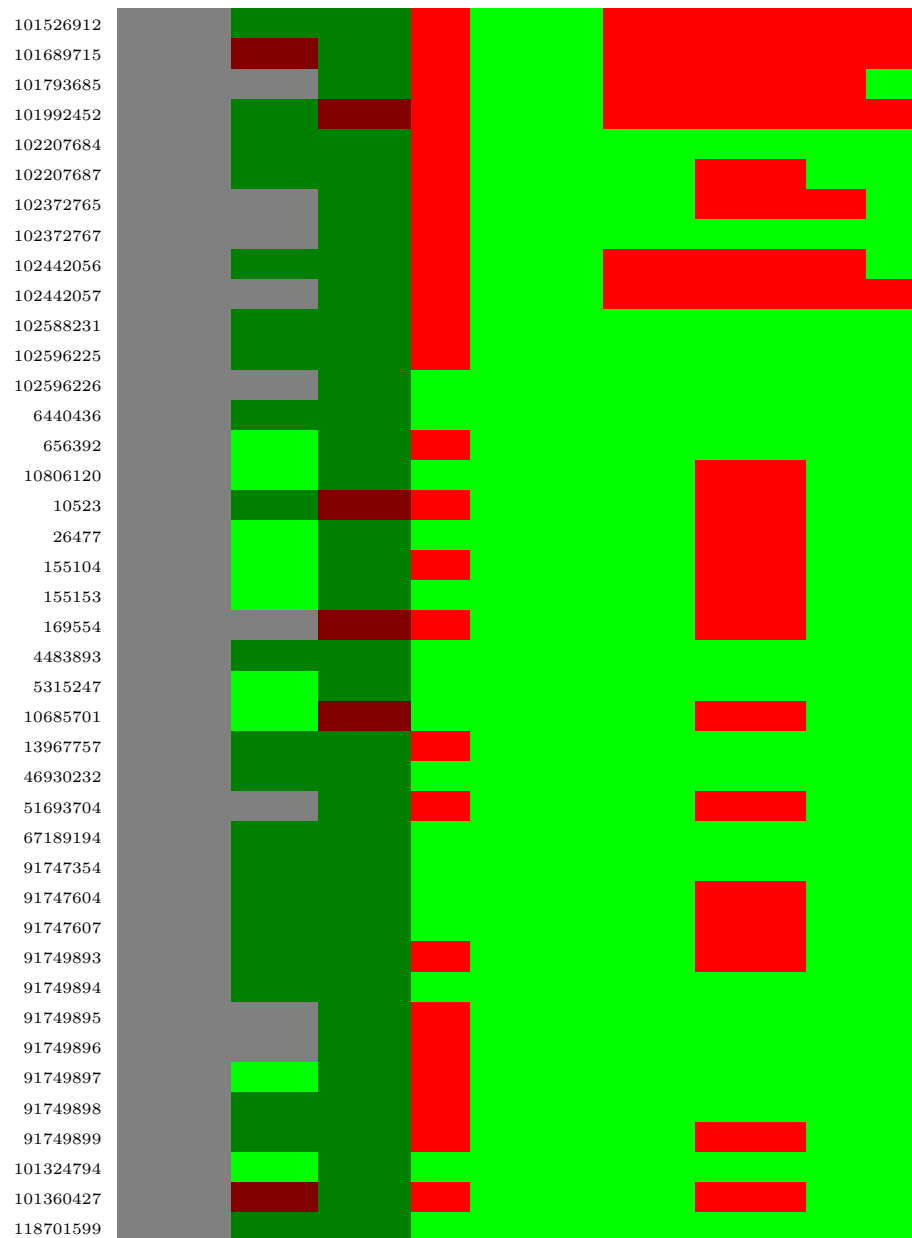








21144858				
21581303				
21626760				
21670206				
22524559				
23305279				
44148183				
46861355				
51413602				
52340564				
52340565				
68380175				
74934296				
91746536				
91746606				
91747012				
91747610				
91747612				
91747938				
91747943				
91749424				
91749426				
91749427				
91749428				
91749429				
91749431				
91749432				
91749433				
91749434				
91749435				
91749436				
91749439				
91749440				
91749448				
91749449				
91749454				
91749889				
91749890				
91753677				
91991897				
92019195				
92233018				
92246526				
92263445				
92263446				
93504569				
98567771				
100916220				
100976533				
101297661				
101324857				
101360989				



269 Table 5 summarises the number of positive and negative mutagenicity predictions for all  
 270 investigated models.

Table 5: Summary of pyrrolizidine alkaloid mutagenicity predictions

Model	Nr.predictions	mutagenic	non-mutagenic
lazar-MP2D (all)	560 (93 %)	111 (20 %)	449 (80 %)
lazar-MP2D (high-confidence)	301 (50 %)	76 (25 %)	225 (75 %)
lazar-PaDEL (all)	600 (100 %)	83 (14 %)	517 (86 %)
lazar-PaDEL (high-confidence)	0 (0 %)	0 (0 %)	0 (0 %)
R-RF	602 (100 %)	18 (3 %)	584 (97 %)
R-SVM	602 (100 %)	11 (2 %)	591 (98 %)
R-DL	602 (100 %)	521 (87 %)	81 (13 %)
Tensorflow-RF	602 (100 %)	186 (31 %)	416 (69 %)
Tensorflow-LR-sgd	602 (100 %)	286 (48 %)	316 (52 %)
Tensorflow-LR-scikit	602 (100 %)	395 (66 %)	207 (34 %)
Tensorflow-NN	602 (100 %)	295 (49 %)	307 (51 %)

For the visualisation of the position of pyrrolizidine alkaloids in respect to the training data set we have applied t-distributed stochastic neighbor embedding (t-SNE, Maaten and Hinton (2008)) for MolPrint2D and PaDEL descriptors. t-SNE maps each high-dimensional object (chemical) to a two-dimensional point, maintaining the high-dimensional distances of the objects. Similar objects are represented by nearby points and dissimilar objects are represented by distant points.

Figure 3 shows the t-SNE of pyrrolizidine alkaloids (PA) and the mutagenicity training data in MP2D space (Tanimoto/Jaccard similarity).

Figure 4 shows the t-SNE of pyrrolizidine alkaloids (PA) and the mutagenicity training data in PaDEL space (Euclidean similarity).

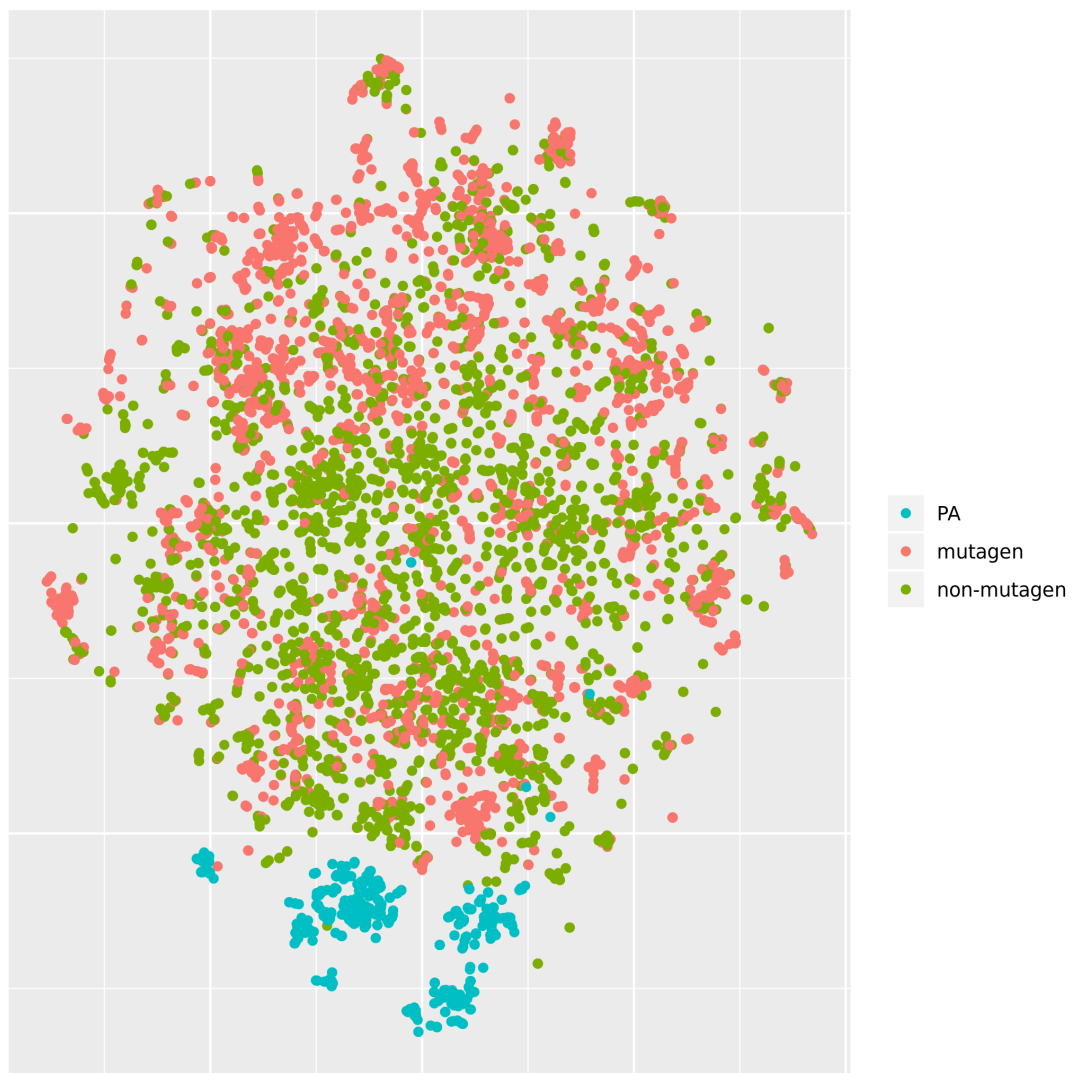


Figure 3: t-SNE visualisation of mutagenicity training data and pyrrolizidine alkaloids (PA)

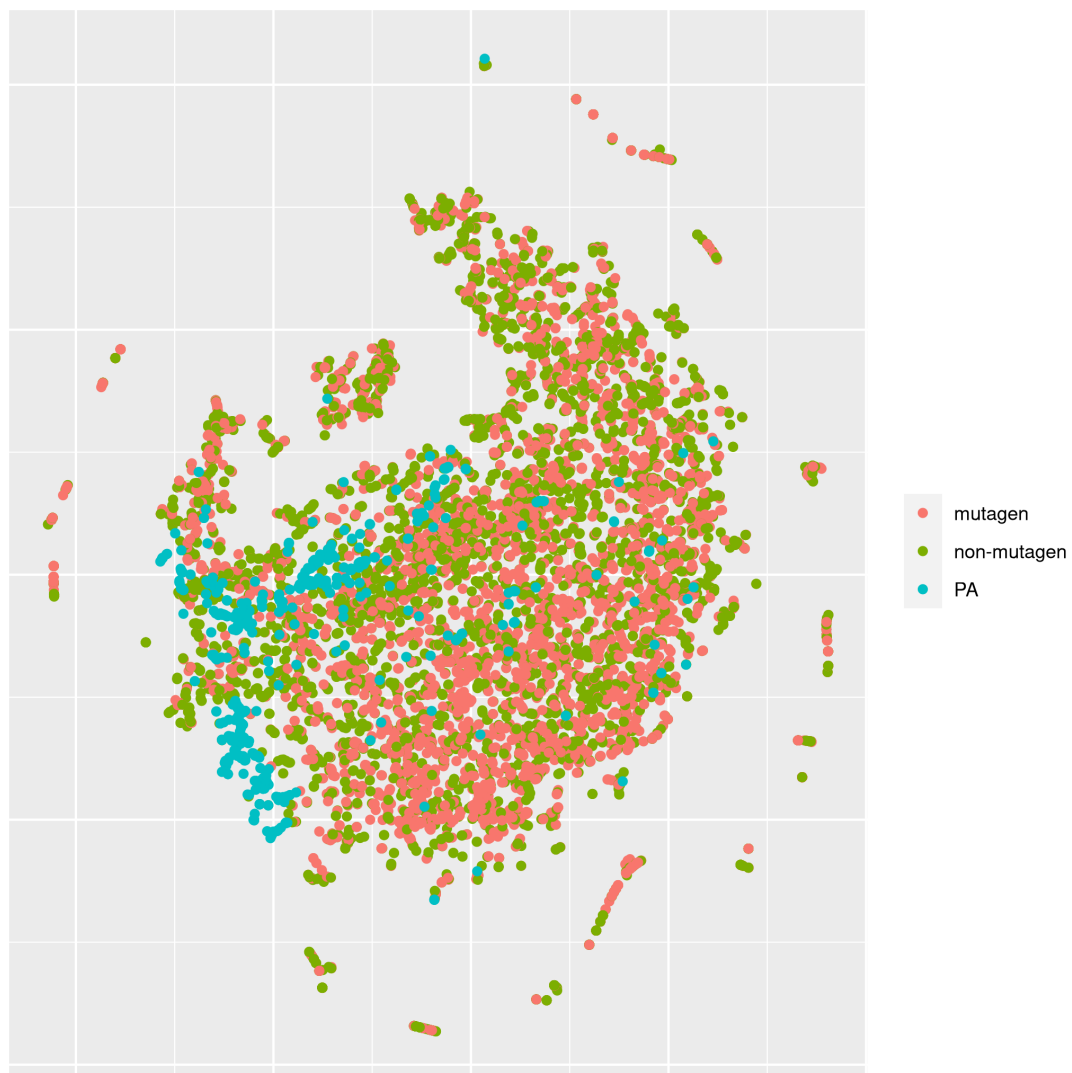


Figure 4: t-SNE visualisation of mutagenicity training data and pyrrolizidine alkaloids (PA)

## Discussion

### Data

A new training dataset for *Salmonella* mutagenicity was created from three different sources (Kazius, McGuire, and Bursi (2005), Hansen et al. (2009), EFSA (2016)). It contains 8309 unique chemical structures, which is according to our knowledge the largest public mutagenicity dataset presently available. The new training data can be downloaded from <https://git.in-silico.ch/mutagenicity-paper/data/mutagenicity.csv>.

### Model performance

Table 1, Table 2, Table 3 and Figure 2 show that the standard **lazar** algorithm (with MP2D fingerprints) give the most accurate crossvalidation results. R Random Forests, Support Vector Machines and Tensorflow models have similar accuracies with balanced sensitivity (true position rate) and specificity (true negative rate). **lazar** models with PaDEL descriptors have low sensitivity and R Deep Learning models have low specificity. The accuracy of **lazar** *in-silico* predictions are comparable to the interlaboratory variability of the Ames test (80-85% according to Benigni and Giuliani (1988)), especially for predictions with high confidence (84%). This is a clear indication that *in-silico* predictions can be as reliable as the bioassays, if the compounds are close to the applicability domain. This conclusion is also supported by our analysis of **lazar** lowest observed effect level predictions, which are also similar to the experimental variability (Helma et al. (2018)).

The lowest number of predictions (4081) has been obtained from **lazar**-PaDEL high confidence predictions, the largest number of predictions comes from Tensorflow models (). Standard **lazar** give a slightly lower number of predictions (7781) than R and Tensorflow models. This is not necessarily a disadvantage, because **lazar** abstains from

305 predictions, if the query compound is very dissimilar from the compounds in the training  
306 set and thus avoids to make predictions for compounds out of the applicability domain.

## 307 Descriptors

308 This study uses two types of descriptors for the characterisation of chemical structures:  
309 *MolPrint2D* fingerprints (MP2D, Bender et al. (2004)) use atom environments (i.e.  
310 connected atom types for all atoms in a molecule) as molecular representation, which  
311 resembles basically the chemical concept of functional groups. MP2D descriptors are  
312 used to determine chemical similarities in the default **lazar** settings, and previous ex-  
313 periments have shown, that they give more accurate results than predefined fragments  
314 (e.g. MACCS, FP2-4).

315 In order to investigate, if MP2D fingerprints are also suitable for global models we have  
316 tried to build R and Tensorflow models, both with and without unsupervised feature  
317 selection. Unfortunately none of the algorithms was capable to deal with the large and  
318 sparsely populated descriptor matrix. Based on this result we can conclude, that Mol-  
319 Print2D descriptors are at the moment unsuitable for standard global machine learning  
320 algorithms.

321 **lazar** does not suffer from the size and sparseness problem, because (a) it utilizes inter-  
322 nally a much more efficient occurrence based representation and (b) it uses fingerprints  
323 only for similarity calculations and not as model parameters.

324 PaDEL calculates topological and physical-chemical descriptors.

325 **TODO: Verena** kannst Du bitte die Deskriptoren nochmals kurz beschreiben

326 *PaDEL* descriptors were used for **lazar**, R and Tensorflow models. All models based on  
327 PaDEL descriptors had similar crossvalidation accuracies that were significantly lower  
328 than **lazar** MolPrint2D results. Direct comparisons are available only for the **lazar**



algorithm, and also in this case PaDEL accuracies were lower than MolPrint2D accuracies.

Based on **lazar** results we can conclude, that PaDEL descriptors are less suited for chemical similarity calculations than MP2D descriptors. It is also likely that PaDEL descriptors lead to less accurate predictions for global models, but we cannot draw any definitive conclusion in the absence of MP2D models.

## Algorithms

**lazar** is formally a *k-nearest-neighbor* algorithm that searches for similar structures for a given compound and calculates the prediction based on the experimental data for these structures. The QSAR literature calls such models frequently *local models*, because models are generated specifically for each query compound. R and Tensorflow models are in contrast *global models*, i.e. a single model is used to make predictions for all compounds. It has been postulated in the past, that local models are more accurate, because they can account better for mechanisms, that affect only a subset of the training data. Our results seem to support this assumption, because standard **lazar** models with MolPrint2D descriptors perform better than global models. The accuracy of **lazar** models with PaDEL descriptors is however substantially lower and comparable to global models with the same descriptors.

This observation may lead to the conclusion that the choice of suitable descriptors is more important for predictive accuracy than the modelling algorithm, but we were unable to obtain global MP2D models for direct comparisons. The selection of an appropriate modelling algorithm is still crucial, because it needs the capability to handle the descriptor space. Neighbour (and thus similarity) based algorithms like **lazar** have a clear advantage in this respect over global machine learning algorithms (e.g. RF, SVM, LR, NN), because Tanimoto/Jaccard similarities can be calculated efficiently with simple set

354 operations.

## 355 **Pyrrolizidine alkaloid mutagenicity predictions**

356 **lazar** models with MolPrint2D descriptors predicted 93% of the pyrrolizidine alkaloids  
357 (PAs) (50% with high confidence), the remaining compounds are not within its applica-  
358 bility domain. All other models predicted 100% of the 602 compounds, indicating that  
359 all compounds are within their applicability domain.

360 Mutagenicity predictions from different models show little agreement in general (table  
361 4). 42 from 602 PAs have non-conflicting predictions (all of them non-mutagenic). Most  
362 models predict predominantly a non-mutagenic outcome for PAs, with exception of the  
363 R deep learning (DL) and the Tensorflow Scikit logistic regression models ( and 66%  
364 positive predictions).

365 R RF and SVM models favor very strongly non-mutagenic predictions (only 3 and 2  
366 % mutagenic PAs), while Tensorflow models classify approximately half of the PAs as  
367 mutagenic (RF 31%, LR-sgd { :n=>602, :mut=>286, :non\_mut=>316, :n\_perc=>100,  
368 :mut\_perc=>48, :non\_mut\_perc=>52 }%, LR-scikit:66, LR-NN:49%). **lazar** models  
369 predict predominately non-mutagenicity, but to a lesser extend than R models (MP2D:20,  
370 PaDEL:14).

371 It is interesting to note, that different implementations of the same algorithm show little  
372 accordance in their prediction (see e.g R-RF vs. Tensorflow-RF and LR-sgd vs. LR-scikit  
373 in Table 4 and Table 5).

374 **TODO Verena, Philipp** habt ihr eine Erklaerung dafuer?

375 Figure 3 and Figure 4 show the t-SNE of training data and pyrrolizidine alkaloids. In  
376 Figure 3 the PAs are located closely together at the outer border of the training set.  
377 In Figure 4 they are less clearly separated and spread over the space occupied by the

378 training examples.

379 This is probably the reason why PaDEL models predicted all instances and the MP2D  
380 model only 560 PAs. Predicting a large number of instances is however not the ultimate  
381 goal, we need accurate predictions and an unambiguous estimation of the applicabil-  
382 ity domain. With PaDEL descriptors *all* PAs are within the applicability domain of  
383 the training data, which is unlikely despite the size of the training set. MolPrint2D  
384 descriptors provide a clearer separation, which is also reflected in a better separation  
385 between high and low confidence predictions in **lazar** MP2D predictions as compared to  
386 **lazar** PaDEL predictions. Crossvalidation results with substantially higher accuracies  
387 for MP2D models than for PaDEL models also support this argument.

388 Differences between MP2D and PaDEL descriptors can be explained by their specific  
389 properties: PaDEL calculates a fixed set of descriptors for all structures, while Mol-  
390 Print2D descriptors resemble substructures that are present in a compound. For this  
391 reason there is no fixed number of MP2D descriptors, the descriptor space are all unique  
392 substructures of the training set. If a query compound contains new substructures,  
393 this is immediately reflected in a lower similarity to training compounds, which makes  
394 applicability domain estimations very straightforward. With PaDEL (or any other pre-  
395 defined descriptors), the same set of descriptors is calculated for every compound, even  
396 if a compound comes from an completely new chemical class.

397 From a practical point we still have to face the question, how to choose model predictions,  
398 if no experimental data is available (we found two PAs in the training data, but this  
399 number is too low, to draw any general conclusions). Based on crossvalidation results  
400 and the arguments in favor of MolPrint2D descriptors we would put the highest trust  
401 in **lazar** MolPrint2D predictions, especially in high-confidence predictions. **lazar** pre-  
402 dictions have a accuracy comparable to experimental variability (Helma et al. (2018))  
403 for compounds within the applicability domain. But they should not be trusted blindly.

404 For practical purposes it is important to study the rationales (i.e. neighbors and their  
405 experimental activities) for each prediction of relevance. A freely accessible GUI for this  
406 purpose has been implemented at <https://lazar.in-silico.ch>.

407 **TODO: Verena** Wenn Du lazar Ergebnisse konkret diskutieren willst, kann ich Dir aus-  
408 fuehrliche Vorhersagen (mit aehnlichen Verbindungen und deren Aktivitaet) fuer einzelne  
409 Beispiele zusammenstellen

## 410 Conclusions

411 A new public *Salmonella* mutagenicity training dataset with 8309 compounds was cre-  
412 ated and used it to train **lazar**, R and Tensorflow models with MolPrint2D and PaDEL  
413 descriptors. The best performance was obtained with **lazar** models using MolPrint2D  
414 descriptors, with prediction accuracies (84%) comparable to the interlaboratory variabil-  
415 ity of the Ames test (80-85%). Models based on PaDEL descriptors had lower accuracies  
416 than MolPrint2D models, but only the **lazar** algorithm could use MolPrint2D descrip-  
417 tors.

418 **TODO: PA** Vorhersagen

## 419 References

- 420 Bender, Andreas, Hamse Y. Mussa, Robert C. Glen, and Stephan Reiling. 2004. "Molec-  
421 ular Similarity Searching Using Atom Environments, Information-Based Feature Selec-  
422 tion, and a Naïve Bayesian Classifier." *Journal of Chemical Information and Computer*  
423 *Sciences* 44 (1): 170–78. <https://doi.org/10.1021/ci034207y>.
- 424 Benigni, R., and A. Giuliani. 1988. "Computer-assisted Analysis of Interlaboratory  
425 Ames Test Variability." *Journal of Toxicology and Environmental Health* 25 (1): 135–48.

426 <https://doi.org/10.1080/15287398809531194>.

427 EFSA. 2011. “Scientific Opinion on Pyrrolizidine Alkaloids in Food and Feed.” *EFSA*  
 428 *Journal*, no. 9: 1–134.

429 ———. 2016. “Guidance on the Establishment of the Residue Definition for Dietary  
 430 Assessment: EFSA Panel on Plant Protect Products and Their Residues (PPR).” *EFSA*  
 431 *Journal*, no. 14: 1–12.

432 Hansen, Katja, Sebastian Mika, Timon Schroeter, Andreas Sutter, Antonius ter Laak,  
 433 Thomas Steger-Hartmann, Nikolaus Heinrich, and Klaus-Robert Müller. 2009. “Bench-  
 434 mark Data Set for in Silico Prediction of Ames Mutagenicity.” *Journal of Chemical*  
 435 *Information and Modeling* 49 (9): 2077–81. <https://doi.org/10.1021/ci900161g>.

436 Helma, Christoph, David Vorgrimmler, Denis Gebele, Martin Gütlein, Barbara Engeli,  
 437 Jürg Zarn, Benoît Schilter, and Elena Lo Piparo. 2018. “Modeling Chronic Toxicity: A  
 438 Comparison of Experimental Variability with (Q)SAR/Read-Across Predictions.” *Fron-*  
 439 *tiers in Pharmacology*, no. 9: 413.

440 Kazius, J., R. McGuire, and R. Bursi. 2005. “Derivation and Validation of Toxicophores  
 441 for Mutagenicity Prediction.” *J Med Chem*, no. 48: 312–20.

442 Maaten, L. J. P. van der, and G. E. Hinton. 2008. “Visualizing Data Using T-Sne.”  
 443 *Journal of Machine Learning Research*, no. 9: 2579–2605.

444 Mattocks, AR. 1986. *Chemistry and Toxicology of Pyrrolizidine Alkaloids*. Academic  
 445 Press.

446 O’Boyle, Noel, Michael Banck, Craig James, Chris Morley, Tim Vandermeersch, and  
 447 Geoffrey Hutchison. 2011. “Open Babel: An open chemical toolbox.” *J. Cheminf.* 3 (1):  
 448 33. <https://doi.org/doi:10.1186/1758-2946-3-33>.

449 Schöning, Verena, Felix Hammann, Mark Peinl, and Jürgen Drewe. 2017. “Editor’s

450 Highlight: Identification of Any Structure-Specific Hepatotoxic Potential of Different  
451 Pyrrolizidine Alkaloids Using Random Forests and Artificial Neural Networks.” *Toxicol.*  
452 *Sci.*, no. 160: 361–70.

453 Yap, CW. 2011. “PaDEL-Descriptor: An Open Source Software to Calculate Molecular  
454 Descriptors and Fingerprints.” *Journal of Computational Chemistry*, no. 32: 1466–74.